

## **Final Report Updated Boundary Conditions for CAMx Modeling**

PREPARED UNDER A CONTRACT FROM THE  
TEXAS COMMISSION ON ENVIRONMENTAL QUALITY

*The preparation of this report was financed through a contract from the State of Texas through the Texas Commission on Environmental Quality. The content, findings, opinions and conclusions are the work of the author(s) and do not necessarily represent findings, opinions or conclusions of the TCEQ.*

Prepared for:

Jim Smith

Texas Commission on Environmental Quality

121 Park 35 Circle MC 164

Austin, TX 78753

Prepared by:

Uarporn Nopmongcol, Jaegun Jung,

Maria Zatko, Greg Yarwood

Ramboll Environ

773 San Marin Drive, Suite 2115

Novato, California, 94998

July 2016

06-358540

## CONTENTS

|   |           |
|---|-----------|
| <b>EXECUTIVE SUMMARY</b> .....                          | <b>1</b>  |
| <b>1.0 INTRODUCTION</b> .....                           | <b>4</b>  |
| 1.1 Background.....                                     | 4         |
| 1.2 Purpose and Objectives.....                         | 5         |
| <b>2.0 GEOS-CHEM MODELING DATABASE</b> .....            | <b>6</b>  |
| 2.1 GEOS-Chem Version 10-01 updates .....               | 6         |
| 2.2 Chemical Mechanism .....                            | 7         |
| 2.2.1 GEOS-Chem Benchmark Chemistry .....               | 7         |
| 2.2.2 Iodine Chemistry .....                            | 9         |
| 2.3 Meteorology .....                                   | 10        |
| 2.4 Emissions .....                                     | 11        |
| 2.4.1 Emission Inventories Available in GEOS-Chem ..... | 11        |
| 2.4.2 Data Sources for Emission Projections .....       | 11        |
| 2.4.3 Emission Projection Results .....                 | 12        |
| 2.4.4 Anthropogenic Emission Summaries .....            | 14        |
| 2.4.5 Halogen Emissions .....                           | 15        |
| 2.5 Implementation of I-species.....                    | 17        |
| <b>3.0 MODELING RESULTS</b> .....                       | <b>19</b> |
| 3.1 Comparison of the full and compact I-chemistry..... | 19        |
| 3.2 2012 Model Results .....                            | 21        |
| 3.3 Analysis of 2017 with 2012 meteorology.....         | 24        |
| <b>4.0 SUMMARY AND RECOMMENDATIONS</b> .....            | <b>26</b> |
| 4.1 Recommendations.....                                | 26        |
| <b>5.0 REFERENCES</b> .....                             | <b>27</b> |

## TABLES

|             |  |    |
|-------------|--|----|
| Table ES-1  | Summary of the full and compact iodine chemistry.....                      | 1  |
| Table ES-2. | Anthropogenic emissions by world region in millions of tons per year ..... | 3  |
| Table 2-1.  | Lists of reactions included in the compact iodine mechanism.....           | 9  |
| Table 2-2.  | Projection factors for US NEI emissions .....                              | 12 |

|            |  |    |
|------------|--|----|
| Table 2-3. | Anthropogenic emissions by world region in 2012.....       | 14 |
| Table 2-4. | Anthropogenic emissions by world region in 2017.....       | 15 |
| Table 2-5. | Changes in anthropogenic emissions in 2017 from 2012. .... | 15 |
| Table 2-6. | Global annual emissions of halomethanes. ....              | 16 |

## FIGURES

|              |   |    |
|--------------|---|----|
| Figure ES-1. | Comparison of maximum 8-hour ozone in the 2012 base case from the current study and the previous TCEQ's 2012 GEOS-Chem simulation (current - previous) in June (left) and July (right).....   | 2  |
| Figure ES-2. | Comparison of monthly maximum 8-hour ozone in the 2017 and 2012 base case in June (left) and July (right). ....   | 3  |
| Figure 1-1.  | TCEQ 36/12/4 km CAMx nested modeling grids, from: <a href="http://www.tceq.texas.gov/airquality/airmod/rider8/modeling/domain">http://www.tceq.texas.gov/airquality/airmod/rider8/modeling/domain</a> . ....  | 5  |
| Figure 2-1.  | Illustration of the UCX scheme for stratospheric ozone available in GEOS-Chem. ....   | 8  |
| Figure 2-2.  | Schematic representation of iodine and bromine chemistry for the simulation "Br+I".....   | 10 |
| Figure 2-3.  | World regions used adjust emissions by year.....  | 13 |
| Figure 2-4.  | Global sea water concentration of chlorophyll-a (mg/m <sup>3</sup> ) in June 2012 from MODIS satellite data. Note that chlorophyll-a also is detected in freshwater lakes. ....   | 16 |
| Figure 3-1.  | Difference in the highest MDA8 ozone in August, 2012 (left and right) due to oceanic emissions and reactions of iodine compounds (with iodine – without iodine) from compact I-chemistry simulation (left) and full I-chemistry simulation (right)..... | 20 |
| Figure 3-2.  | Average monthly IO concentrations in August, 2012 from full I-chemistry simulation (top left), condensed I-chemistry simulation (top right) and difference from compact chemistry (full – compact; bottom). ....  | 20 |
| Figure 3-3.  | Maps of the monthly maximum 8-hour ozone in the 2012 base case from the current study (left), previous TCEQ's 2012 GEOS-Chem simulation (middle), and their differences (right).....  | 23 |
| Figure 3-4.  | Monthly (May-August) average vertical concentration profiles of ozone at Trinidad Head up to 30 km (left) and zoom-in 10 km (right). ....   | 24 |

Figure 3-5. Maps of monthly maximum 8-hour ozone in the 2017 base case (left) and their differences from the 2012 base case (right) in the TCEQ 36 km domain.....25

## EXECUTIVE SUMMARY

Global models are used to prepare boundary conditions for regional-scale air quality modeling, including the Texas Commission on Environmental Quality (TCEQ) Continental US (CONUS) domain. Regional modeling for the Texas Gulf Coast region is strongly affected by ozone over predictions in air arriving from the Gulf of Mexico. Ozone predictions along the Gulf Coast depend upon emissions and chemistry over the Gulf of Mexico and boundary conditions (BCs) entering the regional modeling domain. Previous modeling with the Comprehensive Air quality Model with extensions (CAMx) has reduced the ozone bias through addition of halogen chemistry, especially iodine, which depletes ozone within the marine boundary layer.

This purpose of this study was to provide TCEQ with updated BCs for the CAMx regional modeling. We added iodine chemistry to the latest version (v10-01) of the Goddard Earth Observing System Chemistry (GEOS-Chem) global model. The standard chemical mechanism in this version, referred to as the “benchmark mechanism,” includes bromine and chlorine but lacks iodine chemistry. The GEOS-Chem model was run with iodine emissions and chemistry included for a base year (2012) and a future year (2017). Two iodine mechanisms were tested: 1) compact iodine chemistry recently implemented in CAMx (Yarwood et al., 2016) and 2) full iodine chemistry described by Sherwen et al. (2016). Table ES-1 summarizes these two mechanisms. Both mechanisms reduce ozone across the CONUS domain with larger reductions over oceans. The full I-chemistry reduces peak daily maximum 8-hour average (MDA8) ozone in August by up to 15 ppb, while the condensed mechanism reduced MDA8 ozone by up to 7 ppb. Measurements of iodine oxide (IO) concentrations over the Gulf are needed to better constrain the iodine chemistry and emissions.

**Table ES-1 Summary of the full and compact iodine chemistry.**

| Mechanism         | Full                  | Compact   |
|-------------------|-----------------------|---|
| Source            | Sherwin et al. (2016) | CAMx condensed I-chemistry<br>Yarwood et al. (2016) |
| # gas rxn         | 29                    | 11  |
| # photolysis rxn  | 14                    | 9   |
| # of species      | 20                    | 16  |
| Heterogeneous rxn | Yes                   | No  |

We compare peak MDA8 ozone between this study and the previous TCEQ’s 2012 GEOS-Chem simulation. Both simulations are based on GEOS-5 2012 meteorology. In the new simulation, monthly peak MDA8 ozone is mostly lower in the Pacific Ocean and near the southern lateral boundary of the TCEQ’s CAMx CONUS domain. The small magnitude of ozone reductions in the Gulf of Mexico (less than 4 ppb) imply that ozone depletion by halogen chemistry is partly offset by higher ozone production in the new simulation. The new simulation shows more than 90 ppb of peak MDA8 across the eastern US during summer months and is biased high.

According to the model developer, several factors could be contributing to this ozone bias including overstated US emissions, excessive boundary layer vertical mixing, overstated lightning NO<sub>x</sub>. Other potential causes include updates to the GEOS-Chem chemical mechanism such as new isoprene chemistry and changes to NO<sub>x</sub>-recycling from organic nitrates.

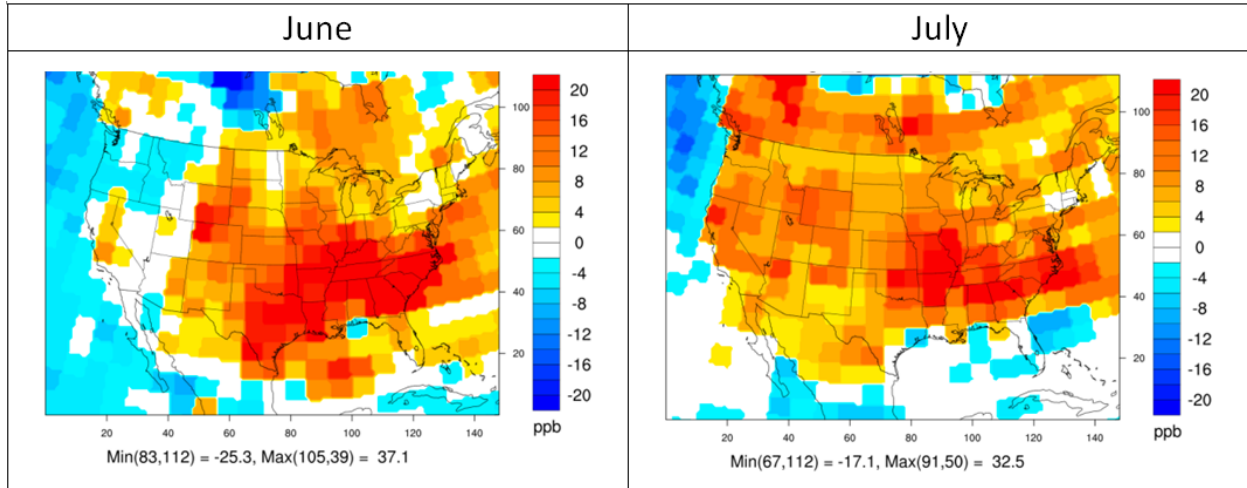


**Figure ES-1. Comparison of maximum 8-hour ozone in the 2012 base case from the current study and the previous TCEQ's 2012 GEOS-Chem simulation ( current - previous) in June (left) and July (right).**

The 2012 and 2017 simulations both used meteorology for 2012 and therefore all changes in ozone were due to differences in emissions between the two years. Emissions for 2017 were determined by applying scaling factors to base year emissions in 6 World regions. US scaling factors were provided by TCEQ. As summarized in Table ES-2, emissions in Asia and MAF (Middle East and Africa) were projected to increase in 2017 while emissions from countries who were members of the Organization for Economic Co-operation and Development in 1990 (OECD90) (US and Western Europe) decreased. Model results from this study suggest that peak MDA8 ozone will be lower in 2017 than 2012 across the US due mainly to reductions in US NO<sub>x</sub> emissions.

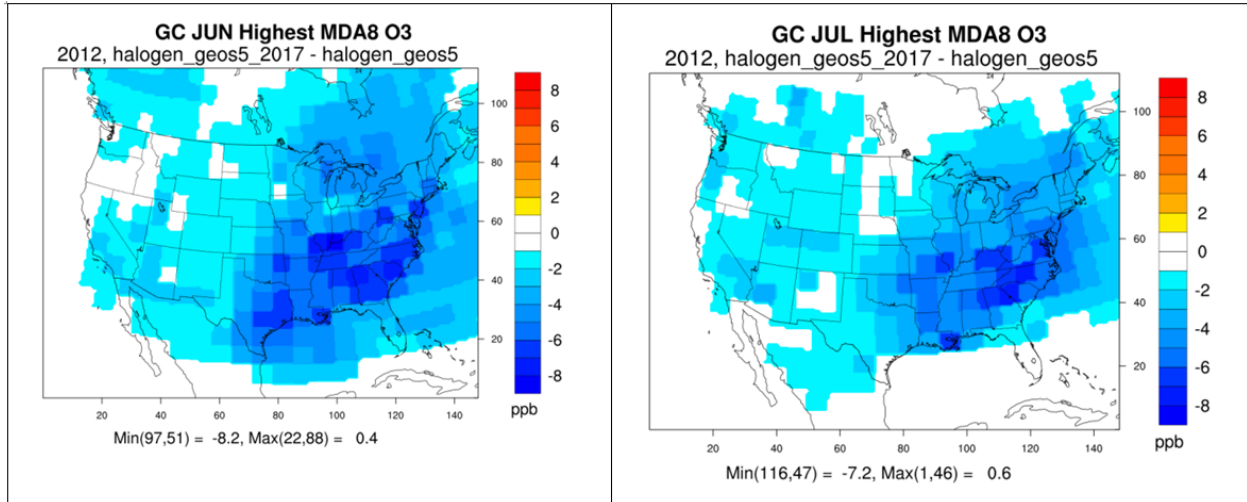


**Figure ES-2. Comparison of monthly maximum 8-hour ozone in the 2017 and 2012 base case in June (left) and July (right).**

**Table ES-2. Anthropogenic emissions by world region in millions of tons per year**

| Region           | NO <sub>x</sub> [MM tons/yr] |      | VOC [MM tons C/yr] |      |
|------------------|------------------------------|------|--------------------|------|
|                  | 2012                         | 2017 | 2012               | 2017 |
| US               | 12.9                         | 10   | 9                  | 8.2  |
| ASIA             | 33                           | 36.4 | 19.6               | 20.9 |
| LAM              | 5.8                          | 6    | 5.1                | 5.2  |
| MAF              | 7.8                          | 8.8  | 8.9                | 9.4  |
| OECD90 except US | 17.4                         | 15.5 | 17.2               | 15.5 |
| REF              | 6.9                          | 7.4  | 7.2                | 7.5  |
| World Shipping   | 18.9                         | 18.9 | 0                  | 0    |
| World Aviation   | 2                            | 2.2  | 0.2                | 0.2  |

## 1.0 INTRODUCTION

### 1.1 Background

The Texas Commission on Environmental Quality (TCEQ) is responsible for developing the Texas State Implementation Plan (SIP) to demonstrate compliance with the National Ambient Air Quality Standard (NAAQS) for ozone. In 2015, the ozone NAAQS was lowered to 70 parts per billion (ppb) based on the three year running average of the annual fourth highest daily maximum 8-hour average (MDA8) ozone measured at each monitoring location. The ozone concentration in background air entering Texas may be as low as 10 ppb for clean air from the Gulf of Mexico or may approach the level of the NAAQS for air of continental origin. Correctly characterizing background ozone is very important to SIP planning because over-estimating background may indicate deeper local emission reductions than are actually needed to meet the NAAQS.

The TCEQ uses the Comprehensive Air Quality Model with extensions (CAMx; Ramboll Environ, 2016) for ozone SIP modeling. The TCEQ CAMx modeling domain covers most of the Gulf of Mexico (Figure 1-1). CAMx modeling for Texas is strongly affected by ozone over predictions in air arriving along the Texas coast (Smith et al., 2014). Ozone predictions along the coast depend upon emissions and chemistry over the Gulf of Mexico and boundary conditions (BC) entering the modeling domain. CAMx BCs are derived from a global model (such as GEOS-Chem; Yantosca et al., 2015), which also tends to over predict ozone in the Gulf region, as do many other regional and global models (Yarwood et al., 2012).

Iodine compounds emitted from ocean waters such as the Gulf of Mexico can cause ozone depletion of several ppb per day within the marine boundary layer (Mahajan et al., 2010 and references therein). Iodine depletes ozone catalytically, meaning that a single iodine atom can destroy many ozone molecules (Chameides and Davis, 1980; Mahajan et al., 2009). Emissions of inorganic iodine compounds ( $I_2$  and HOI) are caused by deposition of ozone to ocean waters (Carpenter et al., 2013), whereas emissions of organic iodine compounds result from biological processes (Carpenter, 2003). Field study data from Mahajan et al. (2010) show that bromine chemistry operates in synergy with iodine chemistry to double the rate of ozone depletion in the marine boundary layer. Emissions of organic bromine compounds also result from biological processes (Carpenter, 2003), while sea-salt aerosol produced by bubble bursting and wind shear at the ocean surface is the dominant source of inorganic bromine and chlorine (Sander et al., 2003).

Recent improvements to CAMx by Ramboll Environ (Yarwood et al., 2012; 2014; 2016) reduced the bias through addition of halogen chemistry to the Carbon Bond version 6, release 2 chemical mechanism (Yarwood et al., 2012; 2014; 2016; Smith et al., 2015), yet substantial over-prediction is still present. Previously developed BCs did not include the influence of halogen chemistry recently incorporated into the CAMx model and consequently over-predicted concentrations of ozone along the modeling domain boundaries. This study ran GEOS-Chem with halogen chemistry aiming to further reduce bias incidents upon the Texas Gulf Coast.



Figure 1-1. TCEQ 36/12/4 km CAMx nested modeling grids, from: <http://www.tceq.texas.gov/airquality/airmod/rider8/modeling/domain>.

## 1.2 Purpose and Objectives

The goal of this project is to provide updated and improved BCs for the CAMx model by: 1) incorporating halogen emissions in the GEOS-Chem model and 2) conducting GEOS-Chem simulations with halogen chemistry for a base year, 2012, and a future year, 2017, with 2012 meteorology.

In Section 2, we summarize GEOS-Chem configuration, model inputs development, and chemical mechanisms used in this work. The GEOS-Chem standard mechanism includes chemistry for bromine and chlorine but lacks chemistry for iodine. This study added two iodine mechanisms into GEOS-Chem: 1) a compact iodine mechanism developed by Ramboll Environ under TCEQ project FY2016-17 (Yarwood et al., 2016) and 2) a mechanism recently described by Sherwen et al. (2016). We incorporated the emission algorithms for inorganic reactive iodine (I<sub>x</sub>; specifically I<sub>2</sub> and HOI) recently implemented by Prados-Roman et al. (2015). The in-line integration responds to surface layer ozone concentration, wind speed and sea surface temperature as adopted in TCEQ project FY2016-17.

The 2012 and 2017 base case GEOS-Chem results are described in Sections 3. Since 2017 was run with 2012 meteorology, a comparison of the 2012 and 2017 GEOS-Chem results is also included. Section 4 presents our conclusions and recommendations stemming from this project.

## 2.0 GEOS-CHEM MODELING DATABASE

GEOS-Chem version 10-01 was released in June, 2015, and has a different structure from the previous GEOS-Chem version, 9-01-03, which was used to develop previous boundary conditions for the TCEQ's 2006, 2012, and 2018 ozone model (Project FY#13-14; Tai et al., 2014). In this section, we summarize model updates, default chemical mechanism, updated halogen mechanism, model inputs and configurations.

### 2.1 GEOS-Chem Version 10-01 updates

There have been many updates to the model science and structure and bug fixes in Version 10-01. Below are important science and structural updates<sup>1</sup>:

- Emissions
  - HEMCO (the Harvard-NASA Emissions Component) - New emission processing program and NetCDF emissions database
  - Update of biomass burning emissions from GFED3 to GFED4<sup>2</sup> (or FINN)
  - Update of MEGAN biogenic emissions<sup>3</sup>
  - Update of EDGAR global anthropogenic emissions
  - Update of US NEI emissions from 2005 to 2011
  - Update of aircraft emissions from Wang et al. (1998) and Park et al. (2004) to AEIC (Aviation Emissions Inventory Code) v. 2.0
- Chemistry
  - Addition of UCX stratospheric chemistry extension (described in Section 3.1.3)
  - Incorporation of updated isoprene chemistry<sup>4</sup>
  - Update of photolysis mechanism from FAST-J to FAST-JX
  - Inorganic chemistry updates from JPL 06 to JPL 11
  - Update of RO<sub>2</sub>+HO<sub>2</sub> reaction rate
  - Increase of NO<sub>3</sub> aerosol reactive uptake coefficient (gamma) from 1.0x10<sup>-4</sup> to 0.1
  - SOA simulation with semi-volatile POA
  - Improved SOA chemistry and can include aerosol from intermediate volatile organic compounds (IVOCs).

Ramboll Environ fixed a few bugs in this version including a wrong emissions unit in the EDGAR inventory read by HEMCO, an incorrect generation of restart file, too low maximum number of output species. The issues have been reported and confirmed by the GEOS-Chem developers.

---

<sup>1</sup> [http://acmg.seas.harvard.edu/geos/doc/man/appendix\\_10.html](http://acmg.seas.harvard.edu/geos/doc/man/appendix_10.html)

<sup>2</sup> <http://onlinelibrary.wiley.com/doi/10.1002/jgrg.20042/abstract>

<sup>3</sup> [http://wiki.geos-chem.org/MEGAN\\_v2.1\\_plus\\_Guenther\\_2012\\_biogenic\\_emissions](http://wiki.geos-chem.org/MEGAN_v2.1_plus_Guenther_2012_biogenic_emissions)

<sup>4</sup> [http://wiki.seas.harvard.edu/geos-chem/index.php/New\\_isoprene\\_scheme#New\\_reactions](http://wiki.seas.harvard.edu/geos-chem/index.php/New_isoprene_scheme#New_reactions)

## 2.2 Chemical Mechanism

The GEOS-Chem benchmark mechanism version 10-01 includes chemistry for bromine and chlorine but lacks chemistry for iodine. We added two iodine mechanisms into GEOS-Chem: 1) a compact iodine mechanism developed by Ramboll Environ under TCEQ project FY2016-17 and 2) a mechanism recently described by Sherwen et al. (2016).

### 2.2.1 GEOS-Chem Benchmark Chemistry

The Benchmark mechanism is a standard mechanism in GEOS-Chem version 10-01. It includes the Unified Tropospheric–Stratospheric Chemistry Extension (UCX; Eastham et al., 2014) and the updated secondary organic aerosol (SOA) chemistry. The UCX improves stratospheric chemistry but does not track SOA species (more information on the UCX is provided below). The SOA mechanism only treats tropospheric chemistry and does not include iodine species. In previous GEOS-Chem simulations, the SOA mechanism was often selected to provide SOA BCs to regional models. The benchmark mechanism combines reactions from these two mechanisms.

#### 2.2.1.1 UCX Stratospheric

This module is only available in GEOS-Chem version 9-02 or later. The UCX version of GEOS-Chem uses the model's existing gas-phase chemistry in the troposphere, but extends the model to use an adapted version of the stratospheric chemistry of NASA's GMI model above the troposphere and below 0.1 hPa, the approximate pressure of the stratopause. The UCX version of the GMI stratospheric chemical mechanism was updated by Eastham et al. to be consistent with the 2011 JPL Chemical Kinetics and Photochemical Data Evaluation (JPL-10-06; Sander et al., 2011). Eastham et al. added 28 species and 104 kinetic reactions beyond what is in the standard GEOS-Chem model's tropospheric chemistry mechanism (Eastham et al., 2013). There are eight additional heterogeneous reactions and 34 additional photolytic decompositions. The UCX stratospheric chemistry includes full ozone chemistry of NO<sub>x</sub>, ClO<sub>x</sub>, BrO<sub>x</sub>, HO<sub>x</sub> and is outlined in Figure 2-1.

There are a number of enhancements in the UCX relative to the standard GEOS-Chem chemistry (prior to version 10) that reflect differences in stratospheric and tropospheric chemistry:

- The UCX contains an extension (FAST-JX<sup>5</sup> v7.0a) of the Fast-J photolysis scheme used in the standard version of GEOS-Chem. Fast-JX treats photolysis at shorter wavelengths than Fast-J so that wavelengths relevant to stratospheric photolysis are included in the model.
- The standard version of GEOS-Chem does not model atomic oxygen species explicitly because their lifetimes are very short; they are treated as intermediate species only. Because atomic oxygen species are important in stratospheric chemistry, the UCX treats oxygen atoms in two electronic states, O(<sup>3</sup>P) and O(<sup>1</sup>D), as explicit species. Ground state atomic hydrogen (H) and nitrogen (N) are also modeled explicitly.

---

<sup>5</sup> [http://wiki.seas.harvard.edu/geos-chem/index.php/FAST-JX\\_v7.0\\_photolysis\\_mechanism](http://wiki.seas.harvard.edu/geos-chem/index.php/FAST-JX_v7.0_photolysis_mechanism)

- Eastham et al. updated GEOS-Chem's gas phase chemistry mechanism to include more detailed treatments of bromine and chlorine chemistry and also added heterogeneous halogen chemistry.
- The UCX can simulate polar stratospheric clouds (PSCs) and background liquid binary sulfate (LBS) aerosols that are not modeled in the standard version of GEOS-Chem.
- With the new stratospheric chemistry implemented in the UCX, additional emissions and boundary conditions were required. In the UCX, a single surface layer mixing ratio boundary condition is used for  $N_2O$ , chlorofluorocarbons (CFCs), hydro chlorofluorocarbons (HCFCs), halons, carbonyl sulfide (OCS) and long-lived organic chlorine species. The standard version of GEOS-Chem simulates emissions of biogenic bromine species, and this treatment is carried through to the UCX.

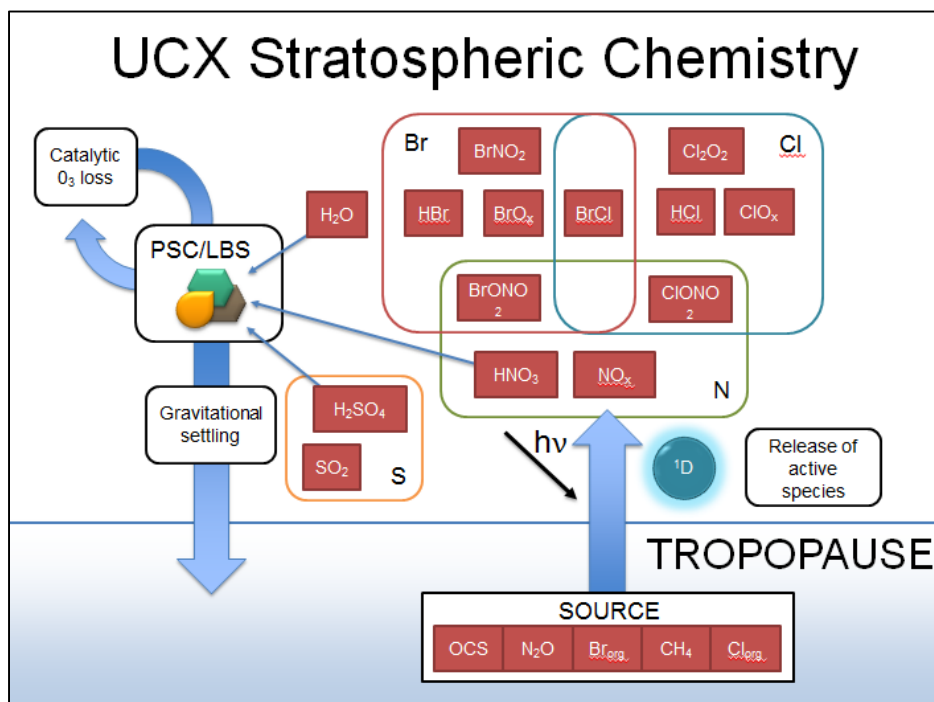


Figure 2-1. Illustration of the UCX scheme for stratospheric ozone available in GEOS-Chem.<sup>6</sup>

Because the UCX is not applied higher in the atmosphere than 0.1 hPa, the chemistry of the mesosphere is not simulated explicitly. Instead, a relaxation to climatology similar to the scheme used for the stratosphere in the standard version of GEOS-Chem (Murray, 2012) is used above 0.1 hPa. This prevents the spurious accumulation in the stratosphere of species that have sinks above the stratopause.

<sup>6</sup> Abbreviations used in Figure 2-1 are: PSC, polar stratospheric clouds; LBS, liquid binary sulfate aerosols;  $O(^1D)$ , oxygen atoms in the singlet D excited electronic state. Source: Weisenstein et al., 2013.

We ran a 6 month spinup period before the beginning of 2012. GEOS-Chem UCX requires at least 5 year spin-up due to the slow rate of circulation in the stratosphere relative to the troposphere. The UCX developer (Sebastian Eastham) provided UCX initial conditions (ICs) that already satisfy the 5-year spin-up requirement.

## 2.2.2 Iodine Chemistry

### 2.2.2.1 Compact Iodine Mechanism

We implemented a compact halogen mechanism for CAMx (referred to as I-16b in Yarwood et al., 2016) plus four additional photolysis reactions for emitted iodine species. The CAMx compact halogen mechanism was recently developed under TCEQ Project FY#16-17 to improve speed in modeling ozone transported into Texas from the Gulf of Mexico (Yarwood et al., 2016). The project identified a sub-group of iodine-related reactions that are consistently the key drivers of ozone depletion across a range of iodine emission and developed a compact 16-reaction mechanism with 9 inorganic iodine species (I-16b mechanism).

**Table 2-1. Lists of reactions included in the compact iodine mechanism.**

| Reactions (I30)   | Note                    |
|---|-------------------------|
| $\text{IO} + \text{NO}_2 = \text{INO}_3$  | I-16b                   |
| $\text{INO}_3 = \text{I} + \text{NO}_3$   | I-16b                   |
| $\text{INO}_3 + \text{H}_2\text{O} = \text{HOI} + \text{HNO}_3$                 | I-16b                   |
| $\text{I}_2 = 2\text{I}$  | I-16b                   |
| $\text{HOI} = \text{I} + \text{OH}$   | I-16b                   |
| $\text{I} + \text{O}_3 = \text{IO}$   | I-16b                   |
| $\text{IO} = \text{I} + \text{O}$   | I-16b                   |
| $\text{IO} + \text{IO} = 0.4\text{I} + 0.4\text{OIO} + 0.6\text{I}_2\text{O}_2$ | I-16b                   |
| $\text{IO} + \text{HO}_2 = \text{HOI}$  | I-16b                   |
| $\text{IO} + \text{NO} = \text{I} + \text{NO}_2$                                | I-16b                   |
| $\text{OIO} = \text{I}$   | I-16b                   |
| $\text{OIO} + \text{OH} = \text{HIO}_3$   | I-16b                   |
| $\text{OIO} + \text{IO} = \text{IXOY}$  | I-16b                   |
| $\text{OIO} + \text{NO} = \text{IO} + \text{NO}_2$                              | I-16b                   |
| $\text{I}_2\text{O}_2 = \text{I} + \text{OIO}$                                  | I-16b                   |
| $\text{I}_2\text{O}_2 + \text{O}_3 = \text{IXOY}$                               | I-16b                   |
| $\text{CH}_3\text{I} = \text{I} + \text{CH}_2\text{O}_2$                        | New photolysis reaction |
| $\text{CH}_2\text{I}_2 = 2\text{I} + \text{CH}_2$                               | New photolysis reaction |
| $\text{CH}_2\text{ICl} = \text{I} + \text{CH}_2\text{Cl}$                       | New photolysis reaction |
| $\text{CH}_2\text{IBr} = \text{I} + \text{CH}_2\text{Br}$                       | New photolysis reaction |

### 2.2.2.2 Full Iodine Mechanism

The science of halogen chemistry in GEOS-Chem has evolved quickly. Parrella et al. (2011) first presented a bromine scheme in GEOS-Chem and its effects on oxidants. Eastham et al. (2014) added a stratospheric bromine and chlorine scheme as currently presented in the UCX mechanism. Recently, Sherwen et al. (2016) incorporated an iodine scheme in the troposphere and found the about 5 ppb decrease of annual mean surface ozone over the Gulf of Mexico by iodine and bromine. The same group is currently coupling their iodine scheme with chlorine



version of meteorology is available (i.e., GEOS-FP<sup>8</sup>), it does not cover our entire modeling period.

## 2.4 Emissions

### 2.4.1 Emission Inventories Available in GEOS-Chem

The CONUS emissions were based on the National Emissions Inventory 2011 (2011 NEI) available in GEOS-Chem<sup>9</sup>. The non-CONUS emissions were based on the Emissions Database for Global Atmospheric Research (EDGAR)<sup>10</sup> and the Reanalysis of the TROpospheric chemical composition between 1960 and 2000 (RETRO)<sup>11</sup> inventory. The RETRO inventory is the default VOC inventory in GEOS-Chem whereas EDGAR version 4.2 is the default inventory for NO<sub>x</sub>, SO<sub>2</sub> and CO.

Other global emission inventories available in GEOS-Chem include:

- MIT Monthly mean aircraft emissions for a baseline year of 2005<sup>12</sup>;
- SO<sub>2</sub> shipping emissions from the ARCTAS<sup>13</sup>;
- CO and NO<sub>x</sub> shipping emissions from ICOADS<sup>14</sup>;
- Anthropogenic ammonia (NH<sub>3</sub>) emissions from the Global Emission Inventory Activity (GEIA) database for a baseline year of 1998 for biofuel sources and 1990 for the rest (Benkovitz et al, 1996);
- Yevich & Logan (2003) inventory for Non-US biofuel emissions;
- Biomass burning emissions based on the Global Fire Emissions Database (GFED) version 4 (monthly emissions are available for 1998-2014, daily and 3-hourly temporal profiles from the most recent year (2011) are applied);
- Tami Bond et al (2007) inventory for biofuel emissions of black carbon and organic carbon;
- Natural emissions (i.e., short-lived bromo-carbon, volcanic SO<sub>2</sub>, biogenic VOCs, soil NO<sub>x</sub>, sea-salt aerosol, oceanic DMS);
- Methane concentrations are defined in GEOS-Chem based on measurements from Climate Monitoring and Diagnostics Laboratory (CMDL) (Dlugokencky et al., 2012).

### 2.4.2 Data Sources for Emission Projections

#### 2.4.2.1 U.S. emission projections

The 2012 emissions use NEI scaling factors available in GEOS-Chem to scale NEI2011 emissions to other years within the period 2006–2013. The factors are from EPA's national-level emissions

<sup>8</sup> <http://wiki.seas.harvard.edu/geos-chem/index.php/GEOS-FP>

<sup>9</sup> [http://wiki.seas.harvard.edu/geos-chem/index.php/EPA/NEI11\\_North\\_American\\_emissions](http://wiki.seas.harvard.edu/geos-chem/index.php/EPA/NEI11_North_American_emissions)

<sup>10</sup> <http://edgar.jrc.ec.europa.eu/index.php>

<sup>11</sup> [http://retro.enes.org/data\\_emissions.shtml](http://retro.enes.org/data_emissions.shtml)

<sup>12</sup> <http://ftp.as.harvard.edu/gcgrid/data/ExtData/HEMCO/AEIC/v2014-10/README>

<sup>13</sup> [http://ftp.as.harvard.edu/gcgrid/data/ExtData/HEMCO/ARCTAS\\_SHIP/v2014-07/README](http://ftp.as.harvard.edu/gcgrid/data/ExtData/HEMCO/ARCTAS_SHIP/v2014-07/README)

<sup>14</sup> [http://ftp.as.harvard.edu/gcgrid/data/ExtData/HEMCO/ICOADS\\_SHIP/v2014-07/README](http://ftp.as.harvard.edu/gcgrid/data/ExtData/HEMCO/ICOADS_SHIP/v2014-07/README)

trends<sup>15</sup>. The NEI2011 was scaled to 2017 based on TCEQ's 2012 to 2017 projections in the TCEQ 36 km domain for all pollutants. Table 2-1 summarizes national scaling factors used in this study.

**Table 2-2. Projection factors for US NEI emissions**

| Species           | 2011 | 2012  | 2017  |
|-------------------|------|-------|-------|
| CO                | 1    | 0.981 | 0.824 |
| NO <sub>x</sub>   | 1    | 0.939 | 0.729 |
| PM <sub>2.5</sub> | 1    | 0.995 | 0.979 |
| SO <sub>2</sub>   | 1    | 0.8   | 0.610 |
| VOC               | 1    | 0.986 | 0.898 |
| NH <sub>3</sub>   | 1    | 0.999 | 0.989 |

#### **2.4.2.2 Emissions Database for Global Atmospheric Research (EDGAR)**

The EDGAR (European Commission, 2011) inventory version 4.2 is the default global inventory in GEOS-Chem for NO<sub>x</sub>, SO<sub>2</sub> and CO. Many global air quality modeling efforts for ozone and aerosols have relied on the EDGAR data base. The inventory is resolved by country, as well as on 1 degree by 1 degree grid, and available from 1970-2005.

#### **2.4.2.3 Representative Concentration Pathway (RCP85) Database**

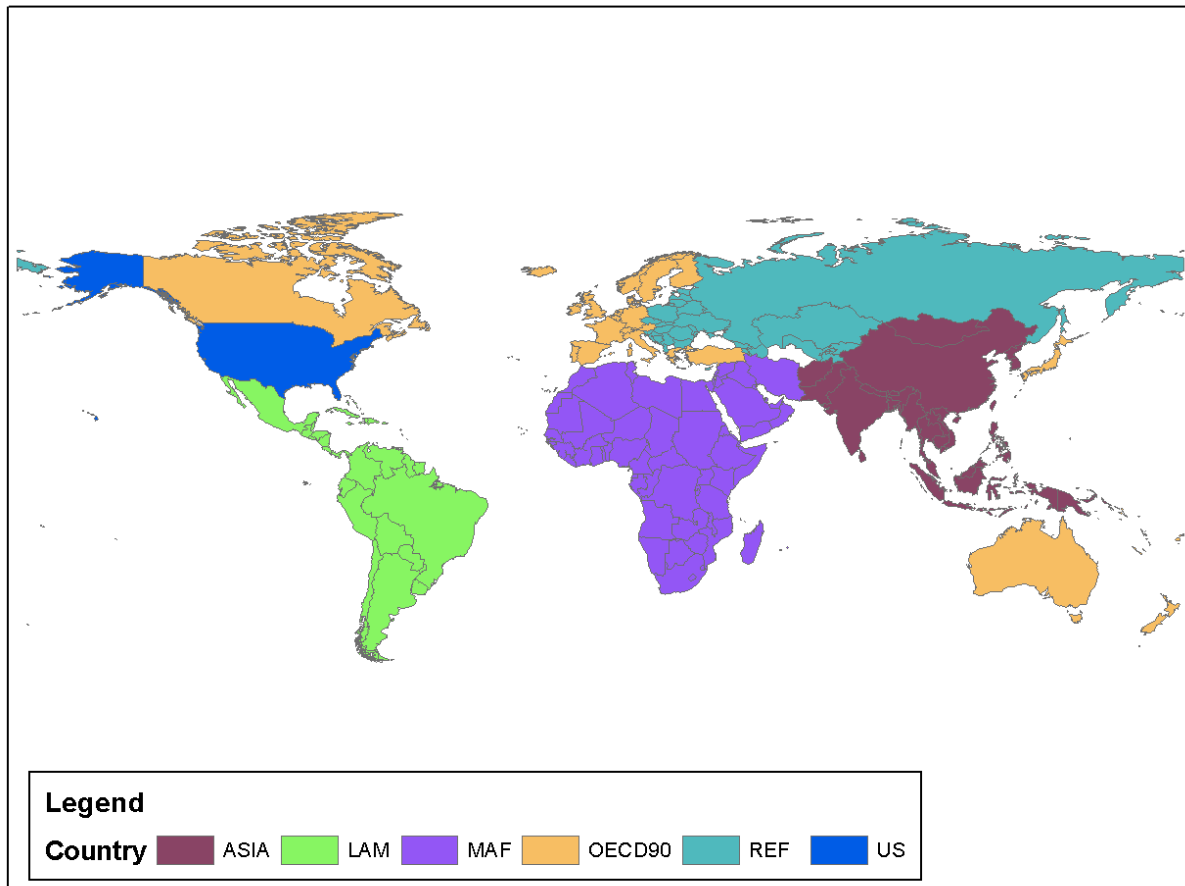
The RCP data<sup>16</sup> serve as input for climate and atmospheric chemistry modeling as part of the Intergovernmental Panel on Climate Change (IPCC) process and other global modeling studies. There are four RCP scenarios available and the RCP85 scenario (Riahi et al., 2007) has the least aggressive emission reductions over the period 2000-2100 and therefore is most likely to represent actual emissions to the time horizon of this project (out to 2017). Anthropogenic emissions in this database are available at a regional level (5 regions total) covering the entire World, and gridded with 0.5x0.5 degree resolution. The RCP85 scenario was used to develop projections from the baseline years (varying by source types) to years 2012 and 2017.

#### **2.4.3 Emission Projection Results**

Anthropogenic emissions were adjusted outside of GEOS-Chem using emission projection factors developed for five World regions (Figure 2-1).

<sup>15</sup> <https://www.epa.gov/air-emissions-inventories/air-pollutant-emissions-trends-data>

<sup>16</sup> <https://tntcat.iiasa.ac.at:8743/RcpDb/dsd?Action=htmlpage&page=welcome>



**OECD90** = Includes the countries who were members of the Organisation for Economic Co-operation and Development in 1990. Countries included in the regions **Western Europe** (Austria, Belgium, Denmark, Finland, France, Germany, Greece, Iceland, Ireland, Italy, Luxembourg, Netherlands, Norway, Portugal, Spain, Sweden, Switzerland, Turkey, United Kingdom), **Northern America** (Canada, United States of America) and **Pacific OECD** (Australia, Fiji, French Polynesia, Guam, Japan, New Caledonia, New Zealand, Samoa, Solomon Islands, Vanuatu); the US is treated separately in this project;

**REF** = Countries from the **Reforming Economies** region (Albania, Armenia, Azerbaijan, Belarus, Bosnia and Herzegovina, Bulgaria, Croatia, Cyprus, Czech Republic, Estonia, Georgia, Hungary, Kazakhstan, Kyrgyzstan, Latvia, Lithuania, Malta, Poland, Republic of Moldova, Romania, Russian Federation, Slovakia, Slovenia, Tajikistan, TFYR Macedonia, Turkmenistan, Ukraine, Uzbekistan, Yugoslavia);

**ASIA** = The countries included in the regions **China +** (China, China Hong Kong SAR, China Macao SAR, Mongolia, Taiwan), **India +** (Afghanistan, Bangladesh, Bhutan, India, Maldives, Nepal, Pakistan, Sri Lanka) and **Rest of Asia** (Brunei Darussalam, Cambodia, Democratic People's Republic of Korea, East Timor, Indonesia, Lao People's Democratic Republic, Malaysia, Myanmar, Papua New Guinea, Philippines, Republic of Korea, Singapore, Thailand, Viet Nam) are aggregated into this region;

**MAF** = This region includes the **Middle East** (Bahrain, Iran (Islamic Republic of), Iraq, Israel, Jordan, Kuwait, Lebanon, Oman, Qatar, Saudi Arabia, Syrian Arab Republic, United Arab Emirates, Yemen) and **African** (Algeria, Angola, Benin, Botswana, Burkina Faso, Burundi, Cote d'Ivoire, Cameroon, Cape Verde, Central African Republic, Chad, Comoros, Congo, Democratic Republic of the Congo, Djibouti, Egypt, Equatorial Guinea, Eritrea, Ethiopia, Gabon, Gambia, Ghana, Guinea, Guinea-Bissau, Kenya, Lesotho, Liberia, Libyan Arab Jamahiriya, Madagascar, Malawi, Mali, Mauritania, Mauritius, Morocco, Mozambique, Namibia, Niger, Nigeria, Reunion, Rwanda, Senegal, Sierra Leone, Somalia, South Africa, Sudan, Swaziland, Togo, Tunisia, Uganda, United Republic of Tanzania, Western Sahara, Zambia, Zimbabwe) countries;

**LAM** = This region includes the **Latin American** countries (Argentina, Bahamas, Barbados, Belize, Bolivia, Brazil, Chile, Colombia, Costa Rica, Cuba, Dominican Republic, Ecuador, El Salvador, Guadeloupe, Guatemala, Guyana, Haiti, Honduras, Jamaica, Martinique, Mexico, Netherlands Antilles, Nicaragua, Panama, Paraguay, Peru, Puerto Rico, Suriname, Trinidad and Tobago, Uruguay, Venezuela);

**US** = United States.

**Figure 2-3. World regions used adjust emissions by year.**

The GEOS-Chem emissions for the CONUS were adjusted to represent 2012 and 2017 using EPA's NEI and TCEQ scaling factors described above. Wild fire emissions were excluded from the projections. Emissions outside the CONUS were adjusted using projections from the RCP85. Since the RCP85 data are only available at 5-10 year intervals (e.g., 2000, 2005, 2010, 2020, etc.) emission projections were linearly interpolated from changes between the two nearest available years.

Natural sources (i.e., volcanic SO<sub>2</sub>, biogenic VOCs, soil NO<sub>x</sub>, sea-salt, lightning NO<sub>x</sub>, mineral dust) are calculated within GEOS-Chem as a function of local values of meteorological variables (temperature, insolation, soil moisture, precipitation, wind speed, convective cloud tops). Default GEOS-Chem procedures were applied to generate 2012 natural emissions. Since 2017 used the same meteorology as 2012, the 2017 natural source emissions are the same as 2012.

#### 2.4.4 Anthropogenic Emission Summaries

A summary of the 2012 and 2017 base case emissions are shown in Table 2-3 and Table 2-4, respectively. Spatial Quality assurance of the emissions projection conducted for the project included the development of emission summaries before and after applying projection factors. HEMCO emission diagnostic output files were inspected to ensure that the emissions were read in correctly.

Table 2-5 lists the difference in emissions from 2012 to 2017. NO<sub>x</sub>, VOC, and CO emissions are projected to increase in Asia and in the Middle East/Africa (MAF) between 2012 and 2017. Emissions in the OECD90 countries (Western Europe, Northern America, and Pacific OECD), including the US, are projected to decrease between 2012 and 2017. In the reforming economies (REF) including Russia minor changes in NO<sub>x</sub>, VOC and CO emissions are expected between 2012 and 2017. SO<sub>2</sub> from shipping emissions is expected to be lower in 2017 due to improved fuel quality.

**Table 2-3. Anthropogenic emissions by world region in 2012.**

| Sources  | World Region        | Emissions (MM Tons/year or MM Tons C/year) |                 |                 |      |
|--|---------------------|--|-----------------|-----------------|------|
|  |                     | CO   | NO <sub>x</sub> | SO <sub>2</sub> | VOC  |
| Total Anthropogenic from NEI   | US                  | 48.1                                       | 12.9            | 5.7             | 9.0  |
| Total Anthropogenic from EDGAR4.2/RETRO/ Xiao C2H6 inventories (excluding aviation and shipping CO/NO <sub>x</sub> /SO <sub>2</sub> emissions) | ASIA                | 182.6                                      | 33.0            | 48.9            | 19.6 |
|  | LAM                 | 43.3                                       | 5.8             | 5.3             | 5.1  |
|  | MAF                 | 72.8                                       | 7.8             | 9.6             | 8.9  |
|  | OECD90 (include US) | 49.0                                       | 17.4            | 11.3            | 17.2 |
|  | REF                 | 19.6                                       | 6.9             | 9.9             | 7.2  |
| Shipping   | World               | 1.1  | 18.9            | 12.6            | 0.0  |
| Aviation   | World               | 0.9  | 2.0             | 0.2             | 0.2  |

**Table 2-4. Anthropogenic emissions by world region in 2017.**

| Sources  | World Region        | Emissions (MM Tons/year or MM Tons C/year) |                 |                 |      |
|--|---------------------|--|-----------------|-----------------|------|
|  |                     | CO   | NO <sub>x</sub> | SO <sub>2</sub> | VOC  |
| Total Anthropogenic from NEI   | US                  | 40.4                                       | 10.0            | 4.4             | 8.2  |
| Total Anthropogenic from EDGAR4.2/RETRO/ Xiao C2H6 inventories (excluding aviation and shipping CO/NO <sub>x</sub> /SO <sub>2</sub> emissions) | ASIA                | 186.8                                      | 36.4            | 50.4            | 20.9 |
|  | LAM                 | 44.7                                       | 6.0             | 4.9             | 5.2  |
|  | MAF                 | 80.6                                       | 8.8             | 10.3            | 9.4  |
|  | OECD90 (include US) | 43.8                                       | 15.5            | 9.5             | 15.5 |
|  | REF                 | 19.1                                       | 7.4             | 9.0             | 7.5  |
| Shipping   | World               | 1.2  | 18.9            | 9.3             | 0.0  |
| Aviation   | World               | 0.9  | 2.2             | 0.3             | 0.2  |

**Table 2-5. Changes in anthropogenic emissions in 2017 from 2012.**

| Sources  | World Region        | Emissions (MM Tons/year or MM Tons C/year) |                 |                 |      |
|--|---------------------|--|-----------------|-----------------|------|
|  |                     | CO   | NO <sub>x</sub> | SO <sub>2</sub> | VOC  |
| Total Anthropogenic from NEI   | US                  | -7.7                                       | -2.9            | -1.4            | -0.8 |
| Total Anthropogenic from EDGAR4.2/RETRO/ Xiao C2H6 inventories (excluding aviation and shipping CO/NO <sub>x</sub> /SO <sub>2</sub> emissions) | ASIA                | 4.2  | 3.4             | 1.5             | 1.3  |
|  | LAM                 | 1.4  | 0.2             | -0.4            | 0.2  |
|  | MAF                 | 7.8  | 1.0             | 0.7             | 0.5  |
|  | OECD90 (include US) | -5.2                                       | -1.8            | -1.8            | -1.7 |
|  | REF                 | -0.5                                       | 0.4             | -0.9            | 0.3  |
| Shipping   | World               | 0.0  | 0.1             | -3.2            | 0.0  |
| Aviation   | World               | 0.1  | 0.2             | 0.0             | 0.0  |

## 2.4.5 Halogen Emissions

### 2.4.5.1 Bromine emissions in GEOS-Chem

Sources of tropospheric bromine species include debromination of sea-salt aerosol, photolysis and oxidation of very short lived (VSL) bromocarbons, and transport from the stratosphere. There are three sources of bromine in GEOS-Chem:

1. Bromomethane (CH<sub>3</sub>Br) concentrations are defined in GEOS-Chem based on measurements from Climate Monitoring and Diagnostics Laboratory (CMDL).
2. Emissions of VSL bromocarbons (CH<sub>2</sub>Br<sub>2</sub> and CHBr<sub>3</sub>) emitted from oceanic macroalgae and phytoplankton are from Liang et al. (2010) and described in Parrella et al. (2012).
3. Sea-salt debromination follows Yang et al. (2005), treating the debromination as an emission of Br<sub>2</sub>, constrained to measured bromide depletion factors relative to seawater for particles in the 1-10 μm diameter range.

### 2.4.5.2 Iodine emissions

#### 2.4.5.2.1 Organic sources

Emissions from seawater of iodomethanes were estimated using the method of Ordóñez et al. (2012) whereby emission rates are proportional to the water content of chlorophyll-a (units of  $\text{mg}/\text{m}^3$ ). The MODIS satellite provides chlorophyll-a data with global coverage as monthly averages, as illustrated in Figure 2-4 for June 2012. Note that the satellite does not provide data for southerly latitudes in this month. We modified HEMCO source codes to read the satellite chlorophyll-concentrations and calculate emission fluxes of halomethans. The halomethane emission factors were calibrated to reproduce global annual emission budgets (Table 2-6).

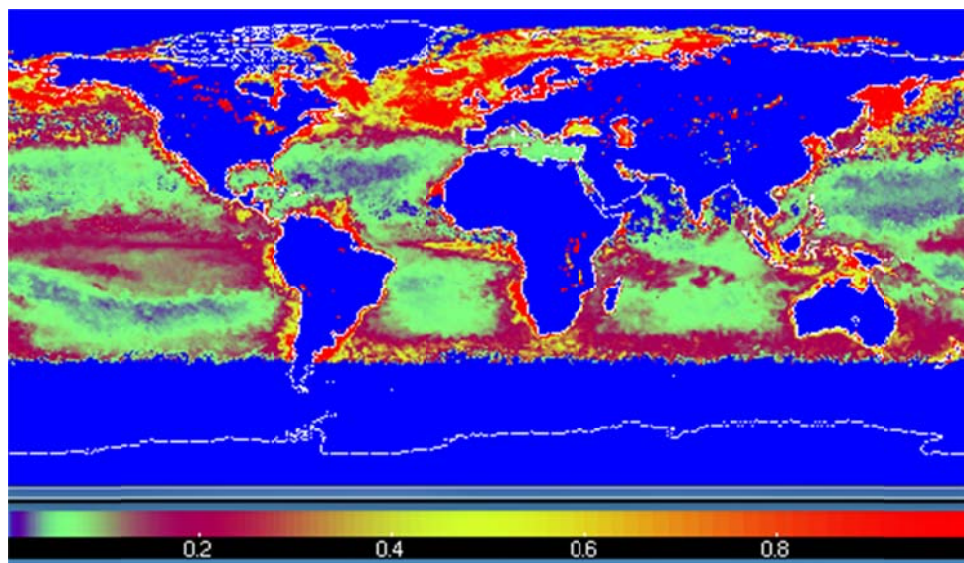


Figure 2-4. Global sea water concentration of chlorophyll-a ( $\text{mg}/\text{m}^3$ ) in June 2012 from MODIS satellite data<sup>17</sup>. Note that chlorophyll-a also is detected in freshwater lakes.

Table 2-6. Global annual emissions of halomethanes.

| Compound         | Formula                        | Global Annual Flux (Gg/year) | Reference           |
|------------------|--------------------------------|------------------------------|---------------------|
| Iodomethane      | $\text{CH}_3\text{I}$          | 213                          | Bell et al., 2002   |
| Diiodomethane    | $\text{CH}_2\text{I}_2$        | 116                          | Ordóñez et al. 2012 |
| Chloriodomethane | $\text{CH}_2\text{I}\text{Cl}$ | 234                          | Ordóñez et al. 2012 |
| Bromiodomethane  | $\text{CH}_2\text{I}\text{Br}$ | 87.3                         | Ordóñez et al. 2012 |

#### 2.4.5.2.2 Inorganic sources

We implemented the emission algorithms for inorganic iodine, specifically for HOI and  $\text{I}_2$ , that were recently implemented by Prados-Roman et al. (2015) into a global chemistry model and by Yarwood et al. (2016) into CAMx. The algorithm is an in-line routine that responds to surface layer ozone ( $\text{O}_3$ ) concentration, wind speed and sea surface temperature (SST).

<sup>17</sup> [ftp://ftp.as.harvard.edu/gcgrid/data/ExtData/CHEM\\_INPUTS/MODIS\\_LAI\\_201204/](ftp://ftp.as.harvard.edu/gcgrid/data/ExtData/CHEM_INPUTS/MODIS_LAI_201204/)

Prados-Roman et al. (2015) used the Community Atmospheric Model with Chemistry (CAM-Chem) global chemistry-climate model (Lamarque et al., 2012) to quantify ocean emissions of inorganic reactive iodine ( $I_x = \text{HOI} + 2 \times I_2$ ) resulting from tropospheric  $O_3$ . They find that long term  $O_3$  enhancement has increased  $I_x$  emissions and in turn accelerated chemical loss of  $O_3$  over the oceans in a negative feedback loop. Following the parameterization developed by Carpenter et al. (2013), CAM-Chem estimates  $I_x$  emissions according to:

$$E(\text{HOI}) = [O_3] \times \left[ 4.15 \times 10^5 \left( \frac{\sqrt{[I_{aq}^-]}}{w} \right) - \left( \frac{20.6}{w} \right) - 2.36 \times 10^4 \sqrt{[I_{aq}^-]} \right]$$

$$E(I_2) = [O_3] \times [I_{aq}^-]^{1.3} \times (1.74 \times 10^9 - 6.54 \times 10^8 \ln w)$$

where the units of  $E$  are  $\text{nmol/m}^2/\text{day}$ ,  $w$  is wind speed (m/s),  $[O_3]$  is surface ozone concentration (ppb), and  $[I_{aq}^-]$  is aqueous iodide concentration ( $\text{mol/dm}^3$ ). Sea surface temperature ( $SST$ , K) is used as the basis for estimating  $[I_{aq}^-]$  (MacDonald et al., 2014):

$$[I_{aq}^-] = 1.46 \times 10^6 e^{\left(\frac{-9134}{SST}\right)}$$

Yarwood et al. (2016) reported strong sensitivity of  $I_x$  emissions to SST and wind speed and that HOI represents 91-99% of the total  $I_x$  emissions flux.

## 2.5 Implementation of I-species

Incorporation of I-chemistry requires a modification of several GEOS-Chem codes and interfaces. Major modification steps include:

Adding new tracers and chemical reactions:

- Assigned specific tracer identification number and molecular weight for new I-species and increased total number of tracers in GEOS-Chem.
- Updated the restart file to include new I-species.
- Incorporated new photochemical, bimolecular, termolecular, and heterogeneous reactions, which required updating the master chemical mechanism and updating the Kinetic PreProcessor (KPP) chemistry solver files.
- Defined absorption cross-section and quantum yield values for each photochemical reaction.
- Defined reactive uptake coefficients for heterogeneous reactions.
- Defined Henry's constant and molar heat of formation required for wet and dry deposition for I-species.
- Added new I-species as diagnostics in order to store concentrations and fluxes to an output file.

#### Adding oceanic emissions of I-species:

- Modified HEMCO emissions interface to calculate in-line organic and inorganic iodine emissions as a function of various parameters described in Section 3.4.5.
- Downloaded and integrated MODIS chlorophyll-a concentrations data
- Modified HEMCO source codes to read-in and store chlorophyll-a data
- Added emitted I-species as diagnostics, which required code modifications at the GEOS-Chem/HEMCO interface level.
- Customized HEMCO diagnostic file to store I-species emissions in an output file

### 3.0 MODELING RESULTS

The iodine mechanisms described in Section 3.2.2 were integrated with the benchmark mechanism in GEOS-Chem version 10-01 and tested using the 2012 meteorology. We first compared and discussed the ozone impacts by I-chemistry below.

#### 3.1 Comparison of the full and compact I-chemistry

We first compare ozone results from two iodine mechanisms – full and compact – to the baseline simulation that has no iodine chemistry. All simulations include bromine chemistry that is part of the benchmark mechanism.

I-chemistry reduces ozone across the CONUS domain (Figure 3-1). Reductions are larger over oceans and tending to be larger at lower latitudes where stronger sunlight enhances photochemistry and warmer water emits more HOI. The full I-chemistry reduces peak daily maximum 8-hour average (MDA8) ozone in August by up to 15 ppb, while the condensed mechanism indicates decrements of up to 7 ppb. Ozone depletion from the two mechanisms has very similar spatial patterns. The full I-chemistry predicts higher IO concentrations than the condensed mechanism (Figure 3-2) which is consistent with generally slower iodine removal in the full I-chemistry. Iodine is removed by conversion to aerosol and the two mechanisms treat this process very differently, with iodine removal being controlled by aerosol processes in the full mechanism but by reactions of small iodine molecules with ozone in the condensed mechanism. Measurements of IO over the Gulf of Mexico are needed to constrain the iodine chemistry and emissions.

The iodine test simulations used MERRA meteorology because it was suggested by the model developers for simulating 2012 and 2013 together with a single source of meteorology. During the course of this study, a publication from the Harvard group (Travis et al., 2016) showed that GEOS-Chem with GEOS-FP meteorology performed well against ozone and NO<sub>x</sub> vertical observations measured over the Gulf of Mexico during SEAC4RS field campaign. However, the GEOS-FP has only become available as of April, 2012. Due to the resource constraints we did not conduct the 2013 simulation. Our 2012 base case modeling used the GEOS-FP's predecessor, GEOS-5, which was also used in the previous TCEQ GEOS-Chem modeling. The base case results are discussed in the next section.

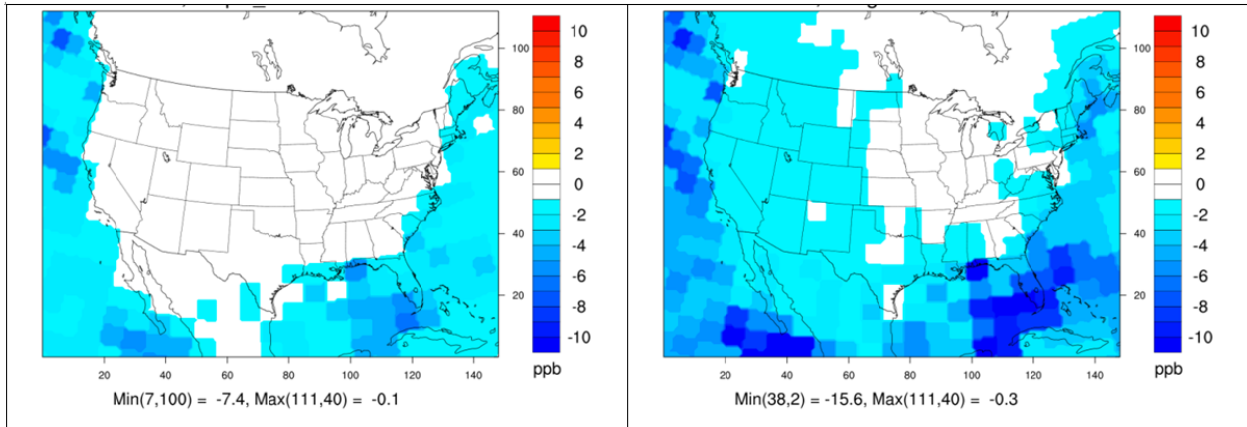


**Figure 3-1. Difference in the highest MDA8 ozone in August, 2012 (left and right) due to oceanic emissions and reactions of iodine compounds (with iodine – without iodine) from compact I-chemistry simulation (left) and full I-chemistry simulation (right).**

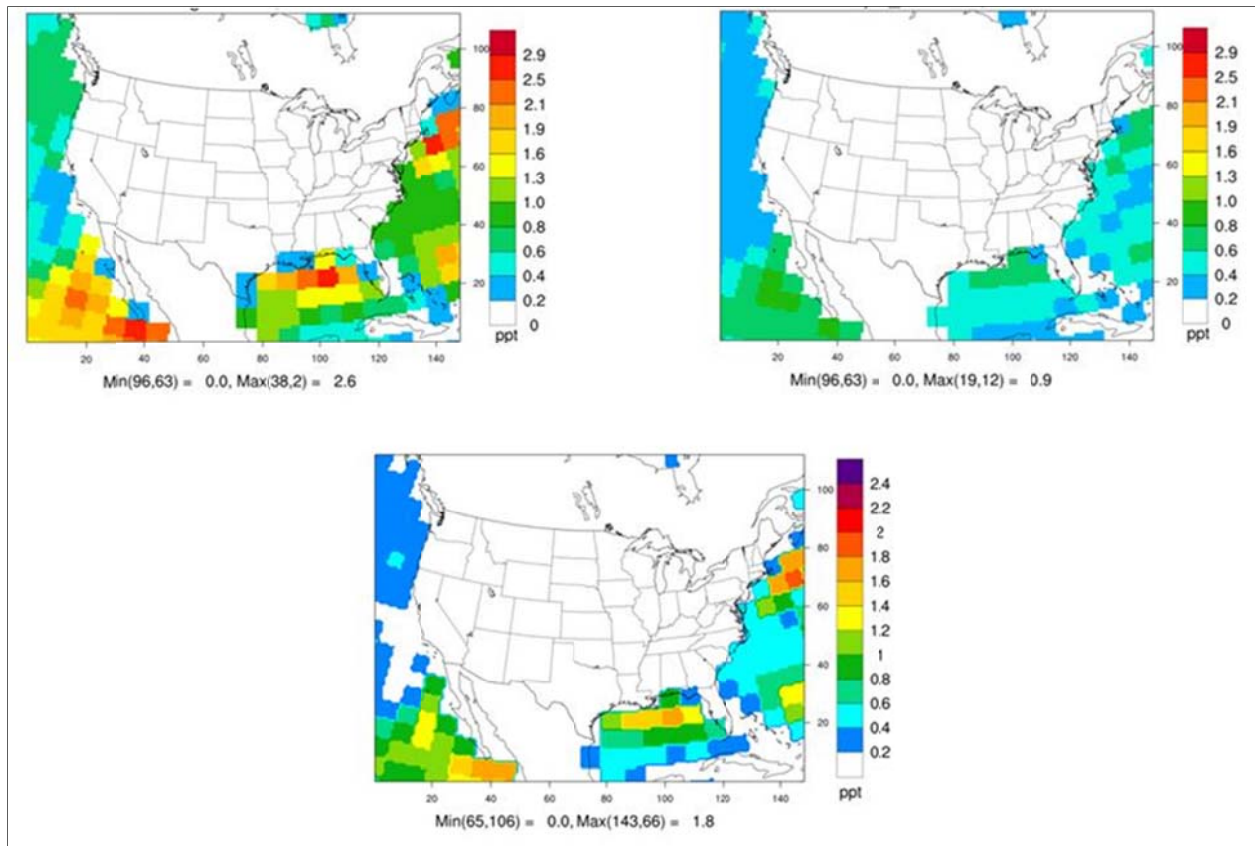


**Figure 3-2. Average monthly IO concentrations in August, 2012 from full I-chemistry simulation (top left), condensed I-chemistry simulation (top right) and difference from compact chemistry (full – compact; bottom).**

### 3.2 2012 Model Results

We compare peak MDA8 ozone between this study and the previous TCEQ's 2012 GEOS-Chem simulation (see Figure 3-3). Both simulations are based on GEOS-5 2012 meteorology. The current base case simulation included halogen chemistry with full I-chemistry described in Section 3.2.2.2. Monthly peak MDA8 ozone is mostly lower in the Pacific Ocean and near the southern lateral boundary of the TCEQ's CAMx CONUS domain. Inland ozone is higher in the current simulation, up to 37 ppb in the eastern US. Higher ozone in the Atlantic Ocean is likely associated with outflow from inland. Small ozone reductions in the Gulf of Mexico (less than 4 ppb) imply that ozone depletion by halogen chemistry is offset by higher ozone production. The current simulation is biased high over land showing more than 90 ppb of peak MDA8 across the eastern US during summer months.

Several factors could be contributing to higher ozone in these 2012 GEOS-Chem simulations than in our previous simulations for TCEQ. Several improvements have been made to GEOS-Chem such as updated isoprene chemistry, more recent US NEI, and others as described in Section 3.1. The updated isoprene chemistry was reported to increase ozone in the Eastern US by 3-5 ppb, but this could be compensated by other updates such as bromine and HO<sub>2</sub> chemistry (Mao et al., 2013). We used hourly US anthropogenic emissions from the 2005 NEI in the previous study and the 2011 NEI in the current study, and adjusted to 2012 using national annual scaling factors. The NO<sub>x</sub> emissions agree within 10% (12.9 compared to 11.7 MM Tons/year). VOC emissions are 70% higher in the current study partly due to oil & gas emissions not included in the 2005 NEI. Higher VOC emissions are not likely the cause of high ozone biases because the eastern US is mostly NO<sub>x</sub>-limited. Harvard's GEOS-Chem simulation using the same 2011 NEI inventory also found high surface ozone biases and concluded that the model biases over the south-eastern US may be due to a combination of excessive NO<sub>x</sub> emissions and excessive boundary layer vertical mixing (Travis et al., 2016). Specifically, they concluded that the NEI NO<sub>x</sub> is 50% too high in the Southeast and nationally.

Recent studies have shown that GEOS-Chem over-estimated lightning NO<sub>x</sub> emissions which contribute to ozone enhancement in the Southwest (Zhang et al., 2014) and in the Gulf of Mexico (Travis et al., 2016). The papers demonstrate that treating the lightning NO<sub>x</sub> yield below 23° to 32° N as tropical (250 mol/flash) rather than extratropical (500 mol/flash) helped improve model ozone performance. This suggested model modification is not included any released versions of GEOS-Chem.

Despite the high bias inland for the new simulation, comparison of the simulated vertical distributions of ozone against observations at Trinidad Head is reasonable (see Figure 3-4). Trinidad head (41.0541°, -124.151°) is a remote site along the northern coast of California. Because of its location, measurements at this site provide an assessment of ozone entering the US with prevailing winds from the Pacific Ocean and so they are useful to evaluate global models.

GC reproduces the strong gradient in ozone above the tropopause with high ozone concentrations (several ppm) in the lower stratosphere which indicates that the UCI chemical

mechanism is describing the chemistry of the lower stratosphere well. This is important because the CAMx top boundary at ~15 km is often in the lower stratosphere. Ozone concentrations entering CAMx through the top boundary should be described well.

In the free troposphere (~1 to ~10 km) GC performance is variable with over and under-predictions depending upon month. An exception is consistent underprediction of ozone between ~1 and 5 km in May to July. Ozone from this height range in the CAMx western BCs can be transported over the Rocky Mountains and influence ground level in the central US (Baker et al., 2015) so this low bias in GC might cause a tendency for CAMx to under-predict the influence of BCs on ozone in Texas during May to July, 2012.

In the marine boundary layer (< 1 km) GC tends to underpredict a consistent observed gradient toward lower ozone at the surface. Potential causes are too little ozone deposition to the ocean, too little chemical destruction of ozone in the marine boundary layer by halogen chemistry, too strong vertical mixing, or a combination of factors. GC bias over the Pacific ocean will not influence Texas because this air is blocked effectively by western mountain ranges. However, if the same problem(s) occur over the Gulf and Atlantic they would influence Texas.

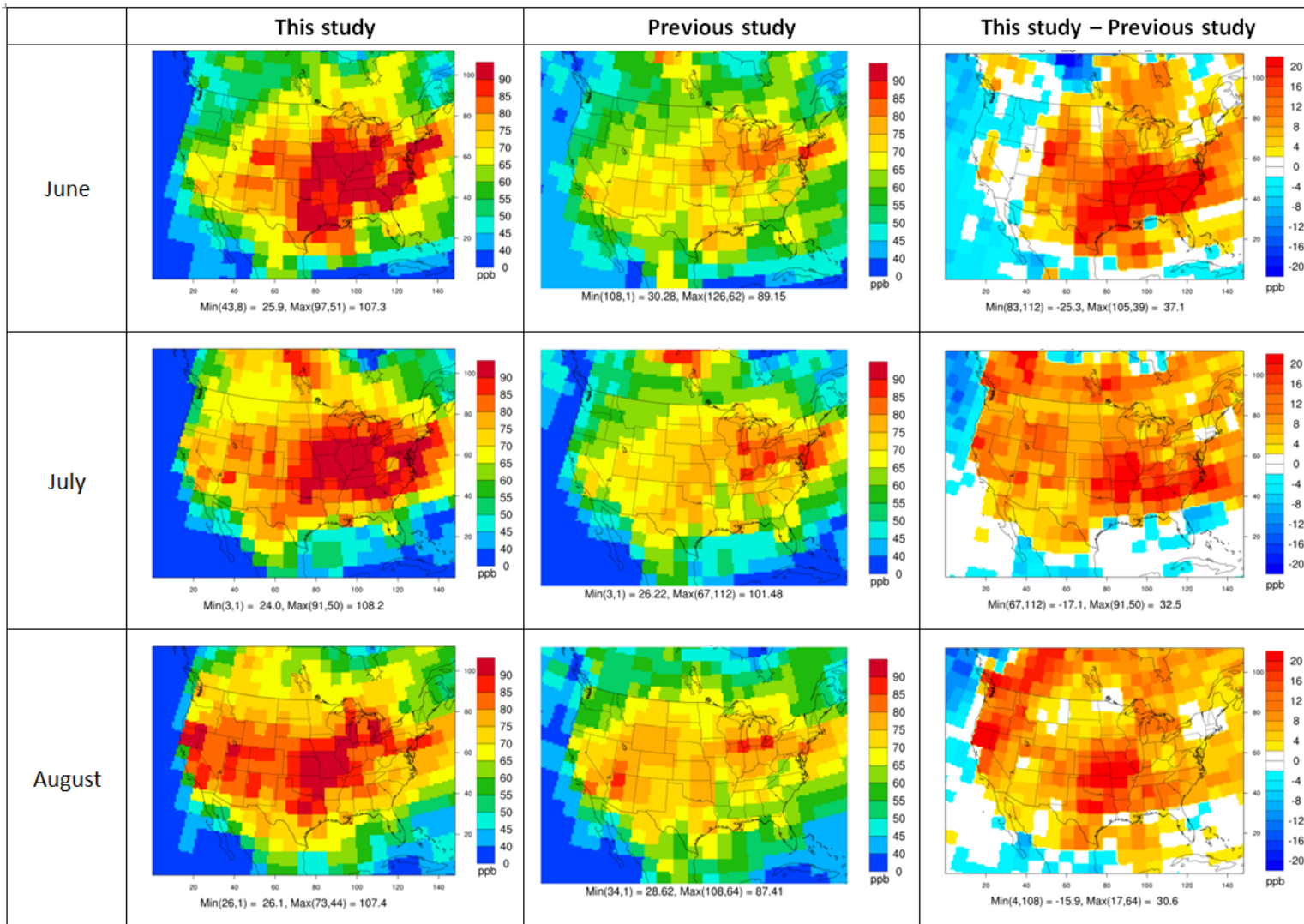


**Figure 3-3. Maps of the monthly maximum 8-hour ozone in the 2012 base case from the current study (left), previous TCEQ’s 2012 GEOS-Chem simulation (middle), and their differences (right).**

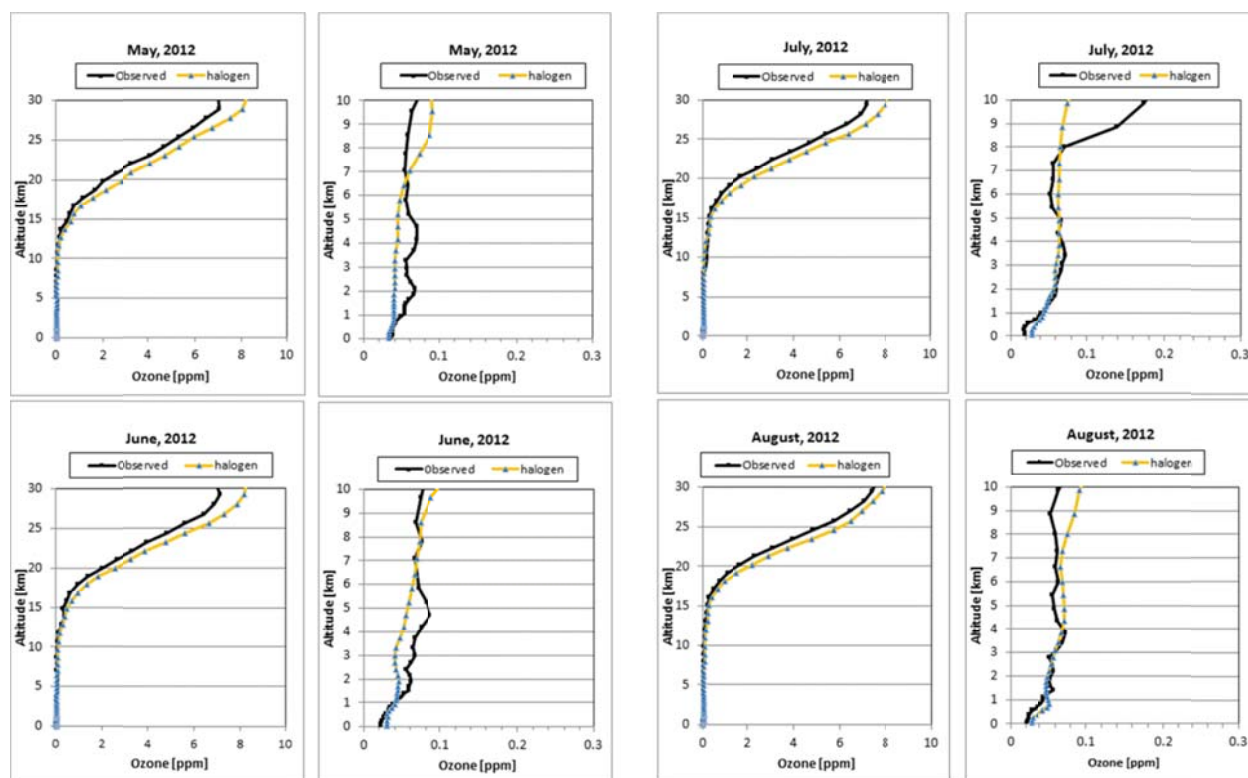


**Figure 3-4. Monthly (May-August) average vertical concentration profiles of ozone at Trinidad Head up to 30 km (left) and zoom-in 10 km (right).**

### 3.3 Analysis of 2017 with 2012 meteorology

GEOS-Chem was run with full I-chemistry to look at ozone in the 2017 future year. Meteorology was the same as 2012 (i.e., GEOS-5) and emissions were scaled to 2017. Natural emissions (e.g., biogenic, fire, LNO<sub>x</sub>, and etc.) are constant from 2012. We compare peak MDA8 ozone between the 2017 and 2012 base case simulations. The monthly peak MDA8 ozone concentrations from the 2017 simulation and comparison to the 2012 simulation are shown in Figure 3-5.

Peak MDA8 ozone is lower in 2017 compared to 2012 across the US due mainly to a reduction of US NO<sub>x</sub> emissions (22%). Differences between 2012 and 2017 are greatest in the southeastern US (up to 8 ppb). Smaller ozone reduction in the west is because the US contribution to total ozone is smaller in the west than the east. Smaller US contribution in the west is due to a combination of higher background ozone and lower emission density on average. Background ozone is expected to be higher in 2017 due to more emissions of ozone precursors originating from Asia in 2017 compared to 2012, NO<sub>x</sub> emissions in Mexico only increase by 3%, thus their contributions to ozone changes are minor.

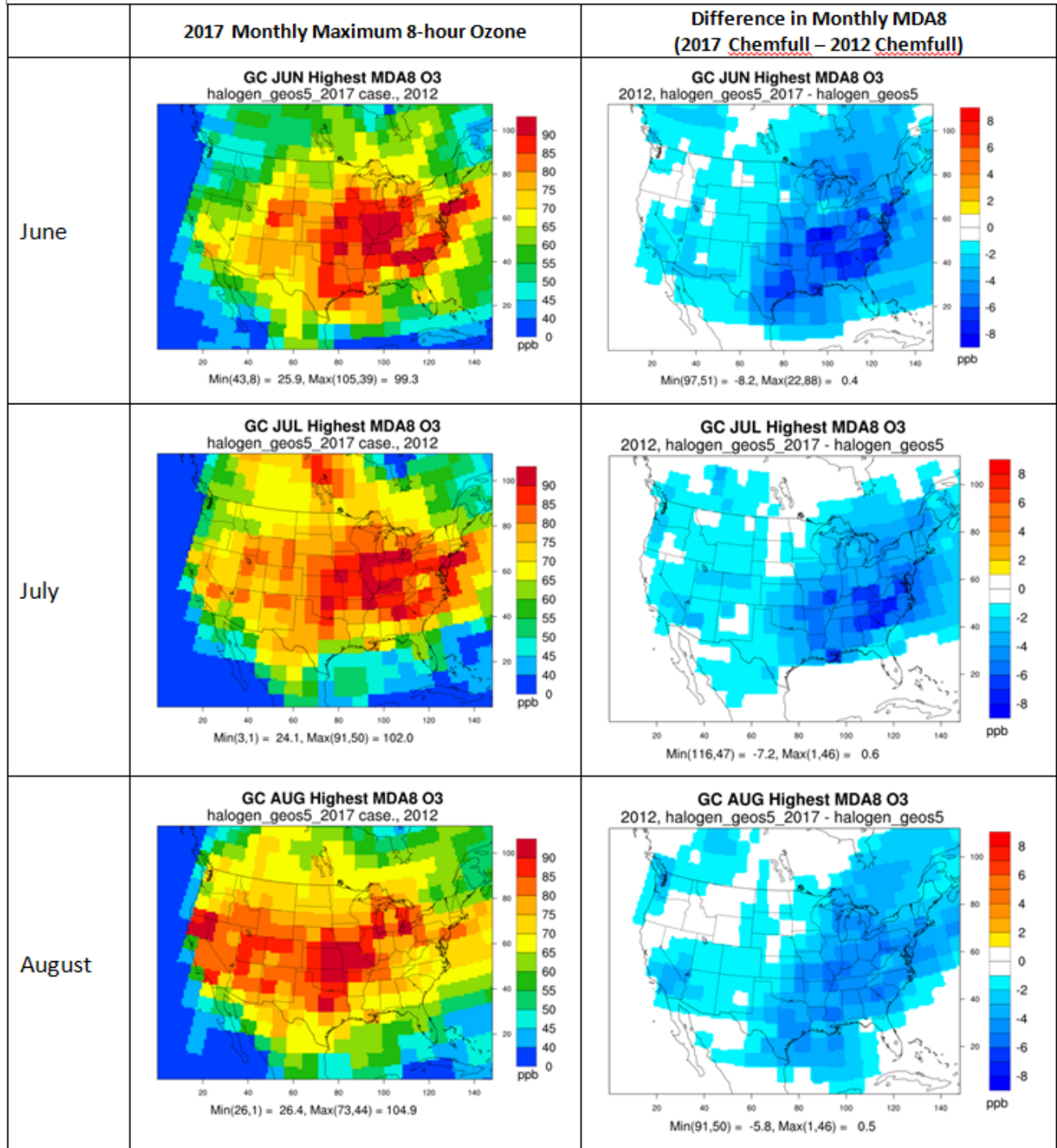


Figure 3-5. Maps of monthly maximum 8-hour ozone in the 2017 base case (left) and their differences from the 2012 base case (right) in the TCEQ 36 km domain.

## 4.0 SUMMARY AND RECOMMENDATIONS

Ramboll Environ implemented iodine emissions and chemistry in the GEOS-Chem global model that TCEQ uses to derive CAMx BCs to improve accuracy in modeling ozone transported into Texas from the Gulf of Mexico. The updates were implemented in the latest version of GEOS-Chem (10-01) which has bromine and chlorine chemistry. We conducted GEOS-Chem simulations with halogen chemistry for a base year, 2012, and a future year, 2017, with 2012 meteorology.

This study implemented iodine emissions within GEOS-Chem. Iodine emission rates from organic sources are proportional to the water content of chlorophyll-a. Inorganic iodine emissions depend upon surface layer ozone concentration, wind speed and sea surface temperature (SST). Both emission pathways are consistent recent iodine implementation in CAMx. CH<sub>3</sub>I emissions from paddy field sources were not included in this work. These sources contribute about 25% to global CH<sub>3</sub>I concentrations (Sherwen et al., 2016), although they are less important in North America.

We incorporated two iodine mechanisms into GEOS-Chem: 1) a compact iodine mechanism available in CAMx and 2) a full mechanism described by Sherwen et al. (2016). Both mechanisms reduce ozone across the CONUS domain with larger reductions over oceans. The full I-chemistry reduces peak MDA8 ozone in August more than the compact mechanism up to 5 ppb in the Gulf. The full I-chemistry is selected for the base case modeling.

The 2012 model results show lower peak MDA8 ozone over water bodies compared to the previous TCEQ's GEOS-Chem 2012 simulation. However, the model exhibits high ozone bias across the eastern US. Small ozone reductions of less than 4 ppb in the Gulf of Mexico suggest that ozone depletion by halogen chemistry is offset by higher ozone contributions from inland. Peak MDA8 ozone is lower in 2017 compared to 2012 across the US due mainly to a reduction of US NO<sub>x</sub> emissions.

### 4.1 Recommendations

Below, we summarize recommendations arising from this study:

- The full iodine chemistry reduces more ozone in the Gulf of Mexico than the compact iodine chemistry. Comparison to measurements of IO at Galveston would be useful for validating models.
- High ozone bias over land in the US should be further examined. Higher inland ozone concentrations compared to previous TCEQ's GEOS-Chem modeling have degraded model performance and may be partially offsetting ozone depletion by halogen chemistry introduced in this work.
- Future GEOS-Chem modeling should modify lightning NO<sub>x</sub> yield as described by Zhang et al., 2014 and Travis et al., 2016.

## 5.0 REFERENCES

- Baker, K.R., C., Emery, P., Dolwick, G., Yarwood. 2015. Photochemical grid model estimates of lateral boundary contributions to ozone and particulate matter across the continental United States. *Atmos. Env.*, 123, pp.49-62.
- Bell, N., L. Hsu, D. J. Jacob, M. G. Schultz, D. R. Blake, J. H. Butler, D. B. King, J. M. Lobert, and E. Maier-Reimer (2002). "Methyl iodide: Atmospheric budget and use as a tracer of marine convection in global models." *Journal of Geophysical Research: Atmospheres* 107, no. D17: ACH-8.
- Benkovitz, C. M., M. T. Scholtz, J. Pacyna, L. Tarrason, J. Dignon, E. C. Voldner, P. A. Spiro, J. A. Logan, and T. E. Graede. 1996. Global gridded inventories of anthropogenic emissions of sulfur and nitrogen, *J. Geophys. Res.*, 101(D22), 29,239-29,253.
- Bond, T.C. et al. 2007. Historical emissions of black and organic carbon aerosol from energy-related combustion, 1850-2000, *Global Biogeochem. Cycles*, 21, GB2018, doi: 10.1029/2006GB002840.
- Carpenter, L.J. 2003. Iodine in the marine boundary layer. *Chemical Reviews*, 103, 4953-4962.
- Carpenter, L.J., S.M. MacDonald, M.D. Shaw, R. Kumar, R.W. Saunders, R. Parthipan, J. Wilson, J.M.C. Plane. 2013. Atmospheric iodine levels influenced by sea surface emissions of inorganic iodine. *Nature Geoscience*, 6, no. 2: 108-111.
- Chameides, W.L., and D.D. Davis. 1980. Iodine: Its Possible Role in Tropospheric Photochemistry. *J. Geophys. Res.*, 85, 7383–7398, doi:10.1029/JC085iC12p07383.
- Dlugokencky, E.J., P.M. Lang, A.M. Croswell, and K.A. Masarie. 2012. Atmospheric Methane Dry Air Mole Fractions from the NOAA ESRL Carbon Cycle Cooperative Global Air Sampling Network, 1983-2011, Version: 2012-09-24.  
<ftp://140.172.192.211/ccg/ch4/flask/month/>.
- Eastham, S., D. K. Weisenstein, S.R.H. Barrett, 2014. Development and evaluation of the unified tropospheric-stratospheric chemistry extension (UCX) for the global chemistry-transport model GEOS-Chem. *Atmos. Env.* 89 (2014) 52-63.  
<http://dx.doi.org/10.1016/j.atmosenv.2014.02.001>.
- Emery, C., Z. Liu., B. Koo, G. Yarwood. 2016. Improved halogen chemistry for CAMx model. Final Report for Work Order No. 582-16-61842-13-FY16-17.
- Lamarque, J.F., L.K. Emmons, P.G. Hess, D.E. Kinnison, S. Tilmes, F. Vitt, C.L. Heald, E.A. Holland, P.H. Lauritzen, J. Neu, J.J. Orlando, P.J. Rasch, G.K. Tyndall. 2012. CAM-chem: description and evaluation of interactive atmospheric chemistry in the Community Earth System Model. *Geosci. Model Dev.*, 5, 369–411, doi:10.5194/gmd-5-369-2012.
- Liang, Q., R.S., Stolarski, S.R., Kawa, J.E., Nielsen, A.R., Douglass, J.M., Rodriguez, D.R., Blake, E.L., Atlas, L.E., Ott. 2010. Finding the missing stratospheric bromine: a global modeling study of CHBr<sub>3</sub> and CH<sub>2</sub>Br<sub>2</sub>, *Atmos. Chem. Phys.*, 10, 2269-2286.

- MacDonald, S.M., J.C. Gómez Martín, R. Chance, S. Warriner, A. Saiz-Lopez, L.J. Carpenter, J.M.C. Plane. 2014. A laboratory characterisation of inorganic iodine emissions from the sea surface: dependence on oceanic variables and parameterization for global modelling. *Atmos. Chem. Phys.*, 14, 5841–5852, doi:10.5194/acp-14-5841-2014.
- Mahajan, A.S., H. Oetjen, A. Saiz-Lopez, J.D. Lee, G.B. McFiggans, J.M.C. Plane. 2009. Reactive iodine species in a semi-polluted environment. *Geophys. Res. Lett.*, 36, L16803, doi:10.1029/2009GL038018.
- Mahajan, A.S., J.M.C. Plane, H. Oetjen, L. Mendes, R.W. Saunders, A. Saiz-Lopez, C.E. Jones, L.J. Carpenter, G.B. McFiggans. 2010. Measurement and modelling of tropospheric reactive halogen species over the tropical Atlantic Ocean. *Atmos. Chem. Phys.*, 10, 4611-4624, 2010 doi:10.5194/acp-10-4611-2010.
- Mao, J., F., Paulot, D.J., Jacob, R.C., Cohen, J.D., Crouse, P.O., Wennberg, C.A., Keller, R.C., Hudman, M. P., Barkley, L.W., Horowitz, L. W. 2013. Ozone and organic nitrates over the eastern United States: Sensitivity to isoprene 25 chemistry, *J. Geophys. Res.: Atmospheres*, 118, 11,256-211,268, doi:10.1002/jgrd.50817.
- Murray, L. 2012. Stratospheric Chemistry in GEOS-Chem. [http://wiki.seas.harvard.edu/geos-chem/index.php/Stratospheric\\_chemistry](http://wiki.seas.harvard.edu/geos-chem/index.php/Stratospheric_chemistry).
- Ordóñez, C., J.-F. Lamarque, S. Tilmes, D.E. Kinnison, E.L. Atlas, D.R. Blake, G. Sousa Santos, G. Brasseur, and A. Saiz-Lopez (2012) "Bromine and iodine chemistry in a global chemistry climate model: description and evaluation of very short-lived oceanic sources," *Atmos. Chem. Phys.*, 12, 1423-1447, doi:10.5194/acp-12-1423-2012.
- Park, R. J., D. J. Jacob, B. D. Field, R. M. Yantosca, and M. Chin, (2004). Natural and transboundary pollution influences on sulfate-nitrate-ammonium aerosols in the United States: implications for policy, *J. Geophys. Res.*, 109, D15204, 10.1029/2003JD004473.
- Parrella, J. P., D.J. Jacob, Q. Liang, Y. Zhang, L. J. Mickley, B. Miller, M. J. Evans et al. 2012. Tropospheric bromine chemistry: implications for present and pre-industrial ozone and mercury, *Atmospheric Chemistry and Physics* 12, no. 15: 6723-6740.
- Prados-Roman, C., C.A. Cuevas, R.P. Fernandez, D.E. Kinnison, J.F. Lamarque, A. Saiz-Lopez. 2015. A negative feedback between anthropogenic ozone pollution and enhanced ocean emissions of iodine. *Atmospheric Chemistry and Physics*, 15(4), 2215-2224.
- Ramboll Environ. 2016. User's Guide: Comprehensive Air Quality Model with extensions, Version 6.30. Available at <http://www.camx.com>
- Riahi, K. Gruebler, A. and Nakicenovic N. 2007. Scenarios of long-term socio-economic and environmental development under climate stabilization. *Tech. Fore. Soc. Change*, 74, 7, 887-935.
- Sherwen, T., M.J., Evans, L.J., Carpenter, S.J., Andrews, R.T., Lidster, B., Dix, T.K., Koenig, R., Sinreich, I., Ortega, R., Volkamer, A., Saiz-Lopez. 2016. Iodine's impact on tropospheric oxidants: a global model study in GEOS-Chem. *Atmospheric Chemistry and Physics*, 16(2), pp.1161-1186.

- Smith, J. H., M. Estes, J. Mellberg, O. Nopmongcol, G. Yarwood. 2015. Addressing model over-prediction of ozone influx from the Gulf of Mexico. Presented at CMAS 2015, <https://www.cmascenter.org/conference/2015/agenda.cfm>.
- Smith, J.H., M. Estes, F. Mercado. 2014. Quantifying Regional Background Ozone for the Houston-Galveston-Brazoria Nonattainment Area. Presented at Midwest and Central States Air Quality Workshop, St. Louis, <http://www.ladco.org/about/general/2014%20Midwest%20Air%20Quality%20Workshop/Presentations.html>.
- Tai, E., U. Nopmongcol, J., Jung, J., King, Y., Alvarez, G., Yarwood. 2014. Foreign contributions to Texas' ozone. Final Report for Work Order No. 582-11-10365-FY13-14
- Travis, K.R., D.J., Jacob, J.A., Fisher, P.S., Kim, E.A., Marais, L., Zhu, K., Yu, C.C., Miller, R.M., Yantosca, M.P., Sulprizio, A.M., Thompson. 2016. NO<sub>x</sub> emissions, isoprene oxidation pathways, vertical mixing, and implications for surface ozone in the Southeast United States, *Atmos. Chem. Phys. Discuss.*, doi:10.5194/acp-2016-110, in review.
- Wang, Y., D.J. Jacob, and J.A. Logan, (1998). Global simulation of tropospheric O<sub>3</sub>-NO<sub>x</sub>-hydrocarbon chemistry, 1. Model formulation, *J. Geophys. Res.*, 103, D9,10,713-10,726.
- Weisenstein, D., S. Eastham, J. Sheng, S. Barrett, T. Peter and D. Keith. 2013. Modeling Stratospheric Aerosols at Background Levels: New Results from SOCOL and GEOS-CHEM. Presentation to SSiRC Meeting, 28-30 October.
- Yang, X., R.A., Cox, N. J., Warwick, J.A., Pyle, G.D., Carver, F.M., O'Connor, N.H., Savage. 2005. Tropospheric bromine chemistry and its impacts on ozone: A model study, *J. Geophys. Res.*, 110, D23311, doi:10.1029/2005JD006244, 2005.
- Yantosca, B., Sulprizio, M., Yannetti, M., Lundgren, L., Xu, J., 2015. GEOS-Chem v10-01 Online User's Guide. Atmospheric Chemistry Modeling Group, School of Engineering and Applied Sciences, Harvard University, Cambridge, MA. (Available at <http://acmg.seas.harvard.edu/geos/doc/man/> )
- Yarwood, G., J. Jung, U. Nopmongcol, C. Emery. 2012. Improving CAMx Performance in Simulating Ozone Transport from the Gulf of Mexico. Final Report for Work Order No. 582-11-10365-FY12-05.
- Yarwood, G., T. Sakulyanontvittaya, U. Nopmongcol, B. Koo. 2014. Ozone Depletion by Bromine and Iodine over the Gulf of Mexico. Final Report for Work Order No. 582-11-10365-FY14-12
- Yevich, R., J. A. Logan. 2003. An assesment of biofuel use and burning of agricultural waste in the developing world, *Global Biogeochem. Cycles*, 17(4), 1095, doi:10.1029/2002GB001952.
- Zhang, L., L., Liu, Y., Zhao, S., Gong, X., Zhang, D.K., Henze, S.L., Capps, T.M., Fu, Q., Zhang, Y., Wang. 2015. Source attribution of particulate matter pollution over North China with the adjoint method. *Environmental Research Letters*, 10(8), p.084011.